Homology modeling of clinically-relevant rilpivirine-resistant HIV-RT variants identifies novel rilpivirine analogs with retained binding affinity against NNRTI-resistant HIV mutations

Charissa Luk*[1,2], Jeslyn Wu*[1,3], Edward Njoo[1]

[1]Department of Chemistry, Biochemistry, & Physical Science, Aspiring Scholars Directed Research Program, Fremont, CA; [2]Bishop O'Dowd High School, Oakland, CA; [3]Mission San Jose High School, Fremont, CA

KEYWORDS non-nucleoside reverse transcriptase inhibitors, reverse transcriptase, high throughput virtual screening, homology modeling, rilpivirine

ABSTRACT: The human immunodeficiency virus (HIV), which affects tens of millions of individuals worldwide, can lead to acquired immunodeficiency syndrome (AIDS). Though there is currently no cure for HIV-infected individuals, the development of small molecule antiretroviral agents has greatly improved the prognosis of infected individuals, especially in developed countries. In particular, compounds such as rilpivirine have been developed as non-nucleoside reverse transcriptase inhibitors (NNRTIs), which allosterically target the reverse transcriptase enzyme in the retrovirus. However, mutations to the reverse transcriptase enzyme threaten to undermine the efficacy of this class of antivirals.Recent advances in computational biophysical modeling enable the structural analyses of such structures without the complications of obtaining crystal structures of such mutations. Here, we employ homology modeling and molecular docking towards the identification of novel rilpivirine analogs that retain high binding affinity to clinically relevant rilpivirine-resistant mutations of the HIV reverse transcriptase enzyme.

Introduction

Human immunodeficiency virus (HIV), which results in acquired immunodeficiency disease (AIDs) affects about 38 million people worldwide as of 2019 [1]. By targeting the CD4+ T cells, the virus causes CD4+ T cell count lower than 200 cells per cubic millimeter of blood as compared to a normal count of 500 to 1600 [2], resulting in a compromised immune system in the host. This loss of the immune system's function increases the host's susceptibility to opportunistic illnesses, cancers, and infectious diseases that would otherwise be well controlled.

While to this day there is no cure for HIV-infected individuals, the development of small molecule therapeutics has advanced antiretroviral therapy (ART) [3], and this is advanced enough to allow infected individuals to live a normal life without developing AIDs. One specific drug class used as HIV treatment is that of non nucleoside reverse transcriptase inhibitors (NNRTIs), which allosterically inhibit the reverse transcriptase (RT) enzyme of HIV [4]. This inhibition of the RT takes advantage of the virus' reliance on RT to complete the transformation of viral RNA into DNA compatible with the system, thereby limiting the virus' ability to replicate within the host. Because RT has no homologs in humans, it is a key target for drug discovery. Rilpivirine (Figure 1a), a second generation diarylpyrimidine (DAPY) NNRTI, has demonstrated superior potency and toxicology profiles compared to previous NNRTI's [5], and was approved for clinical use in the United States in 2011. [5, 6, 7] Like other NNRTI's, rilpivirine binds to the allosteric binding pocket in reverse transcriptase (Figure 1b), where it induces a conformational change in the protein's structure that prevents reverse transcription.

However, the emergence and prevalence of drug-resistant variants of HIV-1 pose a threat to the continued success of antiretroviral therapy [8, 9]. Mainly, mutations in the HIV-1 RT binding pocket have the potential to dramatically decrease

binding affinity, and therefore antiretroviral efficacy, of rilpivirine and other NNRTIs [10], therefore necessitating the continued development and discovery of novel chemical entities which retain activity in viral variants.

Molecular docking allows for predicted binding affinity, and through homology modeling, it is possible to model known structures and mutant structures. Previously, we reported the identification of five top analogs of rilpivirine through a high throughput virtual screen, wherein we described the results of a large-scale high-throughput virtual screen of a library of 2,4-diarylpyrimidines structurally analogous to rilpivirine [11]. Here, we employ homology modeling to model clinically-relevant rilpivirine resistant HIV-1 variants and to predict binding affinity of our reported hit compounds against and provide structural basis for the retention of high binding affinity of our compounds in the presence of key clinical variants through molecular docking experiments. We hypothesize that altering the 4-substituted aniline fragments on our analogs may remove dependence of binding affinity on key residue-ligand interactions, resulting in the retention of high binding affinity to the allosteric pocket of HIV-RT.

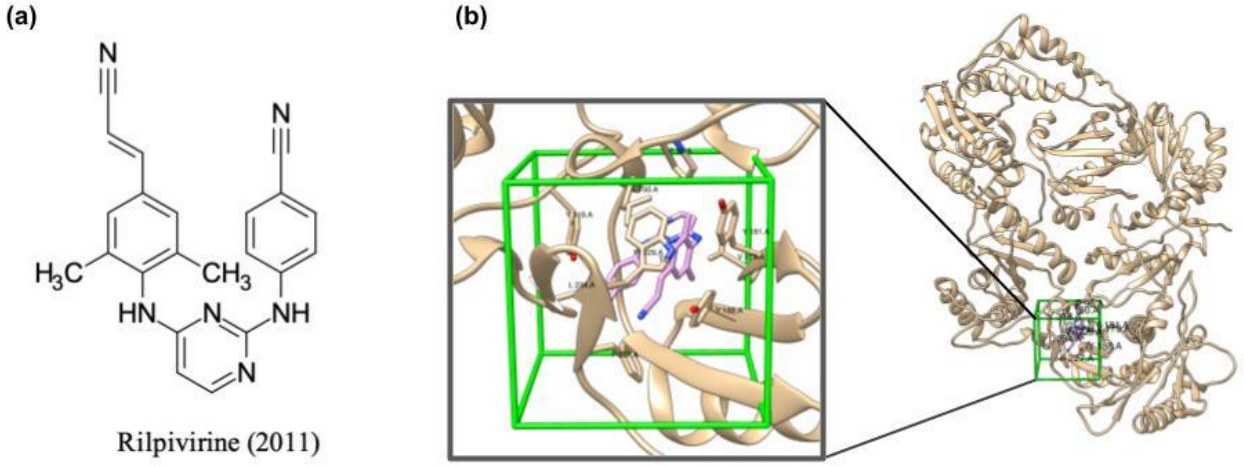

Figure 1 (a) Chemical structure of rilpivirine, a diaryl pyrimidine (DAPY) second generation NNRTI approved for clinical use by the FDA in 2011; (b) crystal structure binding pose (PDB:3MEE) of HIV-1 Reverse Transcriptase in Complex with TMC278 (Rilpivirine). Key residues in the HIV-1 reverse transcriptase allosteric NNRTI- binding pocket include K101, W229, Y181, and Y188.

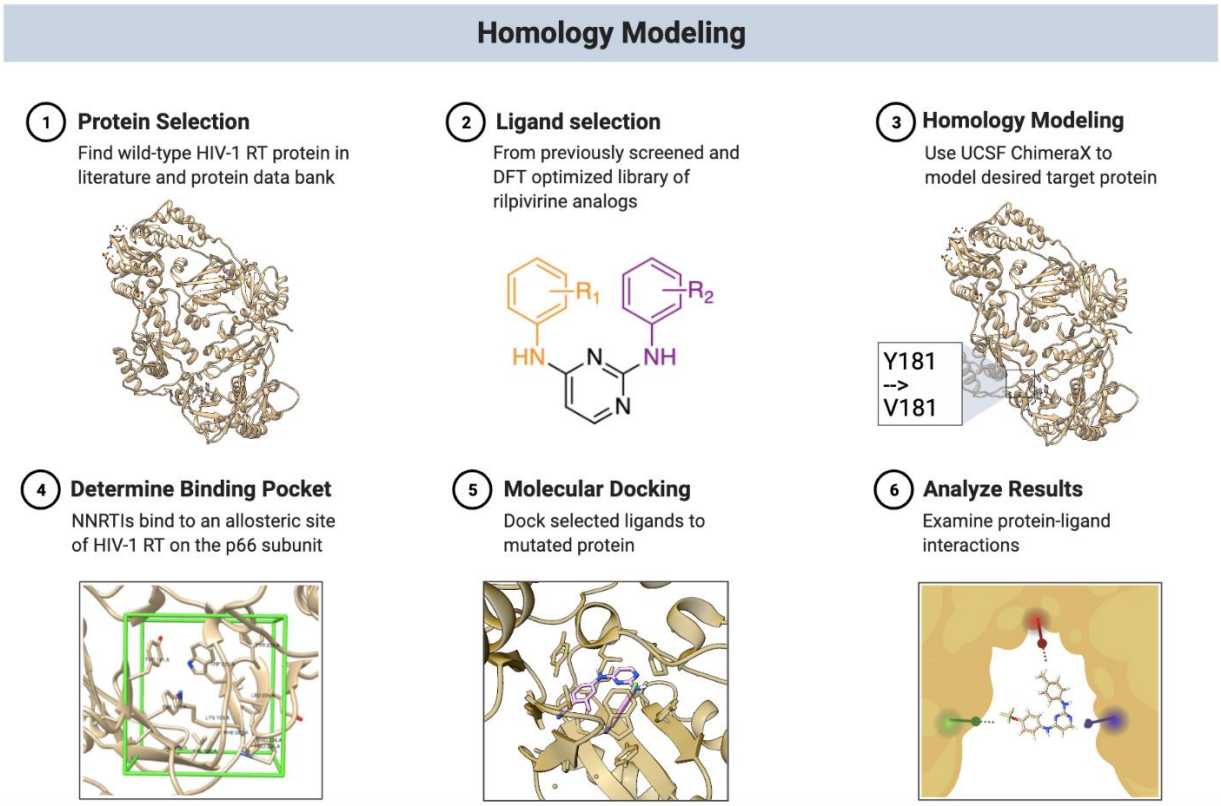

Figure 2 Homology modeling workflow for modeling HIV-1 RT variants.

Residue	L	K	K	V	E	V	Y	Y	H	F	M
Position	100	101	103	106	138	179	181	188	221	227	230
New Residue(s)	I	E	N	A	A	D	C	L	Y	C	I
		P	R		G	L	I				L
					K		V				
					Q						
					R						

Figure 3. Sequence alignment of clinically relevant rilpivirine-resistant mutations.

Results

Homology modeling was utilized to screen clinically relevant NNRTI-resistant variants (Figure 2). A total of 23 structural variants of RT were modeled (Figure 3) 16 of which are associated with decreased rilpivirine efficacy: K101E/P, E138A/G/K/Q/R, V179L, Y181C/I/V, Y188L, H221Y, F227C, and M230I/L, and 5 common double and triple mutants L100I/K103N, L100I/K103R/V179D, K103N/Y181C, V106A/F227L, and V106A/Y181C [10, 12]. The crystal structure of wild-type HIV-RT (PDB: 3MEE) [13] was used as the base scaffold wherewith each variant was separately constructed via single-residue substitution homology models. We used the top five analogs identified in our previously reported HTVS: 4G, 7D, 10D, 7B, and 4E (Fig. 5a), which all exhibited binding affinities comparable to rilpivirine against wild type HIV-1 reverse transcriptase [11]. Binding affinities were calculated from molecular docking experiments using our previously described gridbox parameters based on the crystal structure of HIV-RT liganded with rilpivirine, and the binding affinities of our analogs are reported in a heat map in (Fig. 4a).

E138A/G/K/Q/R and K101E/P Variants

In wild type RT, E138, a negatively charged residue, engages K101 through electrostatic attractions, which is the basis for stabilizing tertiary structure of the allosteric binding pocket. However, in variants wherein glutamic acid mutated to alanine or glycine, which are short, non-polar residues; or arginine or lysine, which are positively charged; or glutamine, which is polar but not anionic at physiological pH, the interaction between E138 and K101 is lost, distorting the binding pocket shape. This loss of structure greatly decreases the binding affinity of rilpivirine from -12.7 kcal/mol against WT to between -8.3 and -9.3 kcal/mol against these variants, and this is consistent with clinical data that suggests that these mutants are resistant to treatment by rilpivirine, as they reduce rilpivirine susceptibility at least 2 to 3-fold [12]. Our analogs, however, retain the same binding affinity as when docked to WT, as they do not rely strongly on the structure of the binding pocket in the inner E138/K101 region, and instead rely mostly on halogen-π interactions with aromatic residues (Fig. 5f).

Mutating K101 to a glutamic acid residue causes a loss of electrostatic interaction with E138 and the two glutamic acid residues repulse each other, resulting in a decreased binding affinity of -8.6 kcal/mol. This is consistent with clinical data where K101E mutation often causes 2.5-3 fold reduced susceptibility to rilpivirine [10]. Mutating to proline, which is a non-polar residue, also causes a loss in binding affinity to -8.3 kcal/mol. Our analogs are able to maintain their binding affinity, again due to the reliance of halogen-π, rather than relying on binding pocket confirmation from the E138/K101 electrostatic interactions like rilpivirine.

K103N and K103N/Y181C Variants

Mutations at lysine 103 cause the binding affinity of rilpivirine to drop significantly to -7.9 kcal/mol. Our analogs experience loss in binding affinity as well, though not as drastic. Notably, analog 7D performs the best, with a binding affinity of -10.8 kcal/mol. The K103N/Y181C double mutant significantly drops the binding affinity of rilpivirine and our analogs to between -9.0 and -8.2 kcal/mol. The decrease in binding affinity of rilpivirine is due to both the loss of the interaction with the positively charged lysine and also loss of the aromatic tyrosine ring. The decrease of our analogs is due to both K103N and Y181C, but mostly due to the Y181C variant, as the loss of the tyrosine residue aromatic ring eliminates the halogen-π interaction which our analogs strongly rely on. The Y181C variant also eliminates critical π-π interactions for rilpivirine and our analogs.

L100I, L100I/K103N, and L100I/K103R/V179D Variants

Leucine is a non-polar, aliphatic residue and forms hydrophobic interactions with the amino nitrile on rilpivirine. Interestingly, the L100I variant causes the binding affinity of analog 4G to be superior to that when docked to WT. Leucine's side chain does not protrude out as much as isoleucine's side chain in the allosteric binding pocket. This mutation increases the distance between the leucine residue at position 100 and rilpivirine in the L100I variant, which causes weaker hydrophobic interactions. For reference, the hydrophobic interaction distance between the nitrogen at position two on rilpivirine's pyrimidine ring and WT L100 is 3.1 Å, whereas the interaction distance between the same nitrogen on rilpivirine to the L100I variant increases to 3.5 Å, resulting in a weaker hydrophobic interaction (Fig. 5b).

It is important to note that L100I rarely occurs on its own, rather, it occurs in combination with K103N, which causes a 10-fold reduced susceptibility to rilpivirine [12]. Against the L100I/K103N variant, the binding affinity of rilpivirine is decreased to -8.1 kcal/mol and the binding affinities for our analogs range from -8.9 to -10.4. Interestingly, in variants that contain the K103N mutation, analog 7D consistently has a superior binding affinity than rilpivirine or our other analogs. The trifluoromethoxy on 7D forms C-H---X interactions with isoleucine 100 at a distance of 3.3 Å and the terminal methyl (-CH3) group on 7D forms electrostatic interactions with mutant K103N at a distance of 3.0 Å, whereas L100I for rilpivirine, it hydrophobic interactions with the amino nitrile on rilpivirine at a distance of 4.4 Å and the amino nitrile interacts with arginine 103 at a distance of 4.9 Å (Fig. 5c). The distances from 7D and the residues are closer than that to analog 7D, causing 7D's superior binding affinity.

The combination of reverse transcriptase associated mutation L100I/K103R/V179D is strongly associated with decreased rilpivirine efficacy, consistent with our findings that rilpivirine's binding affinity decreases to -9.8. Our analogs retain their binding affinity, as their binding is not largely dependent on mutations at the L100 or V179 position.

Y181C/I/V Variants

Y181 in WT HIV-1 RT forms π-π stacking with the aromatic ring of our analogs and halogen-π interactions with the trifluoromethoxy group of our analogs. Thus, mutations at this position, especially Y181V, are observed to be detrimental to the binding affinity of rilpivirine, which is -4.9 kcal/mol, and to our analogs, which range from -5.6 to -4.7 kcal/mol. This is consistent with the reported 10 to 15-fold decrease in rilpivirine susceptibility seen in patients with the Y181V mutation [10]. The loss of the aromatic tyrosine ring in mutations eliminates potential for critical π-π stacking interactions. It also eliminates the halogen-π interaction with the trifluoromethoxy group and tyrosine 181 critical to the success of our analogs.

Additionally, mutant Y181V caused significantly lower binding affinity for rilpivirine and our analogs compared to mutant Y181I, in which our analogs and rilpivirine retained most of their binding affinity. Valine has a shorter side chain compared to isoleucine, which could explain the more significant decrease in binding affinity of the Y181V variant.

Mutant Y181C is reported to reduce rilpivirine susceptibility 3-fold [12], consistent with the docking results for rilpivirine, which was -10.8 kcal/mol. Our analogs had binding affinities similar to rilpivirine with to Y181C despite the loss of π-π interactions because the trifluoromethoxy on our analogs is able to form orthogonal multipolar interactions [14] with the sulfur on cysteine 181, with the distance from the closest fluorine measuring 3.2 Å, which albeit weak, fits into criteria for fluorine–sulfur contacts (2.8–3.4 Å) in experimentally observed protein structures [15]. The other two fluorines on the trifluoromethoxy group are too far, with distances between 4.0-4.8 Å, decreasing the potential for F-S interactions which causes decreased binding affinity for our analogs. It is important to note that the binding pose of rilpivirine and our analogs are similar (Fig. 5d), showing that they are able to form similar interactions that confer similar binding affinities.

Y188L Variant

The Y188L mutant is known to decrease rilpivirine susceptibility 6-fold [10], which is in line with our findings

that this mutant causes rilpivirine to have a reduced binding affinity of -8.3 kcal/mol, while analog 7B retains the best binding affinity at -10.3 kcal/mol. Analog 7B is the only analog without a trifluoromethoxy group, as it does not rely as strongly on halogen-π interactions with tyrosine 188 like our other analogs. Instead, the aromatic ring of 7B is able to form C-H---π interactions with leucine 188 at a distance of 3.5 Å and retain most of its binding affinity (Fig. 5e).

(a)

Mutations	Rilpivirine	4G	7D	10D	7B	4E
wild type	-12.7	-12.8	-12.5	-12.5	-12.4	-12.3
E138A	-9.3	-12.8	-12.5	-12.5	-12.4	-10.6
E138G	-9.3	-12.8	-12.5	-12.5	-12.4	-11.9
E138K	-9.2	-12.8	-12.5	-12.5	-12.4	-11.9
E138Q	-8.3	-12.8	-12.5	-12.5	-12.4	-11.9
E138R	-9.2	-12.8	-12.4	-12.5	-12.4	-11.9
F227C	-9.1	-12.6	-12.2	-12.1	-11.5	-11.9
H221Y	-9.3	-12.8	-12.5	-12.5	-12.4	-12
K101E	-8.6	-12.8	-12.4	-12.4	-12.3	-11.9
K103N	-8.3	-12.2	-11.8	-11.7	-11.4	-11.1
K103N/Y181C	-7.9	-8.7	-10.2	-8	-9.8	-8.5
K101P	-8.6	-8.9	-9	-8.3	-8.3	-8.2
L100I	-8.8	-13.1	-12.6	-12.8	-12.2	-11.9
L100I/K103N	-8.1	-9.5	-10.4	-8.9	-9.9	-9
L100I/K103R/V179D	-9.8	-12.8	-12.3	-12.3	-12.3	-11.9
M230I	-9.3	-12.9	-12.5	-12.5	-12.4	-12
M230L	-9.3	-12.9	-12.5	-12.5	-12.4	-11.9
V106A/F227L	-10.3	-12.1	-11.9	-12	-11.8	-11.6
V106A/Y181C	-10.7	-11	-10.7	-10.6	-9.7	-10.2
V179L	-9.6	-12.6	-12.3	-12.2	-12.3	-11.9
Y181C	-10.8	-10.9	-10.7	-10.3	-9.5	-10.5
Y181I	-10	-10.7	-10.6	-10.2	-9.1	-10.5
Y181V	-4.9	-5.3	-5.6	-5.4	-4.7	-5.4
Y188L	-8.3	-11.3	-11	-10.3	-11.9	-10.4

(b)

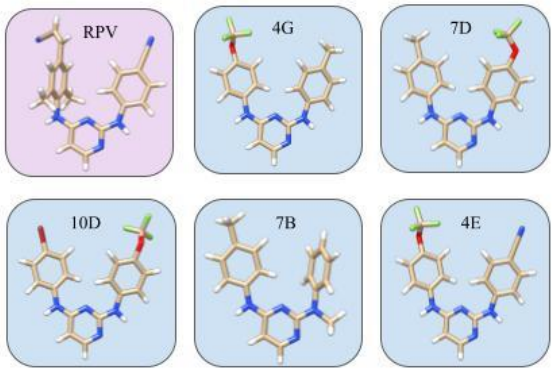

Figure 4. (a) Heat map of computational binding affinities (reported in kcal/mol) from molecular docking experiments against key HIV-RT mutants, color coded by binding affinity values, and (b) DFT-optimized 3D structures of rilpivirine and five top analogs identified from our previously published high throughput virtual screen

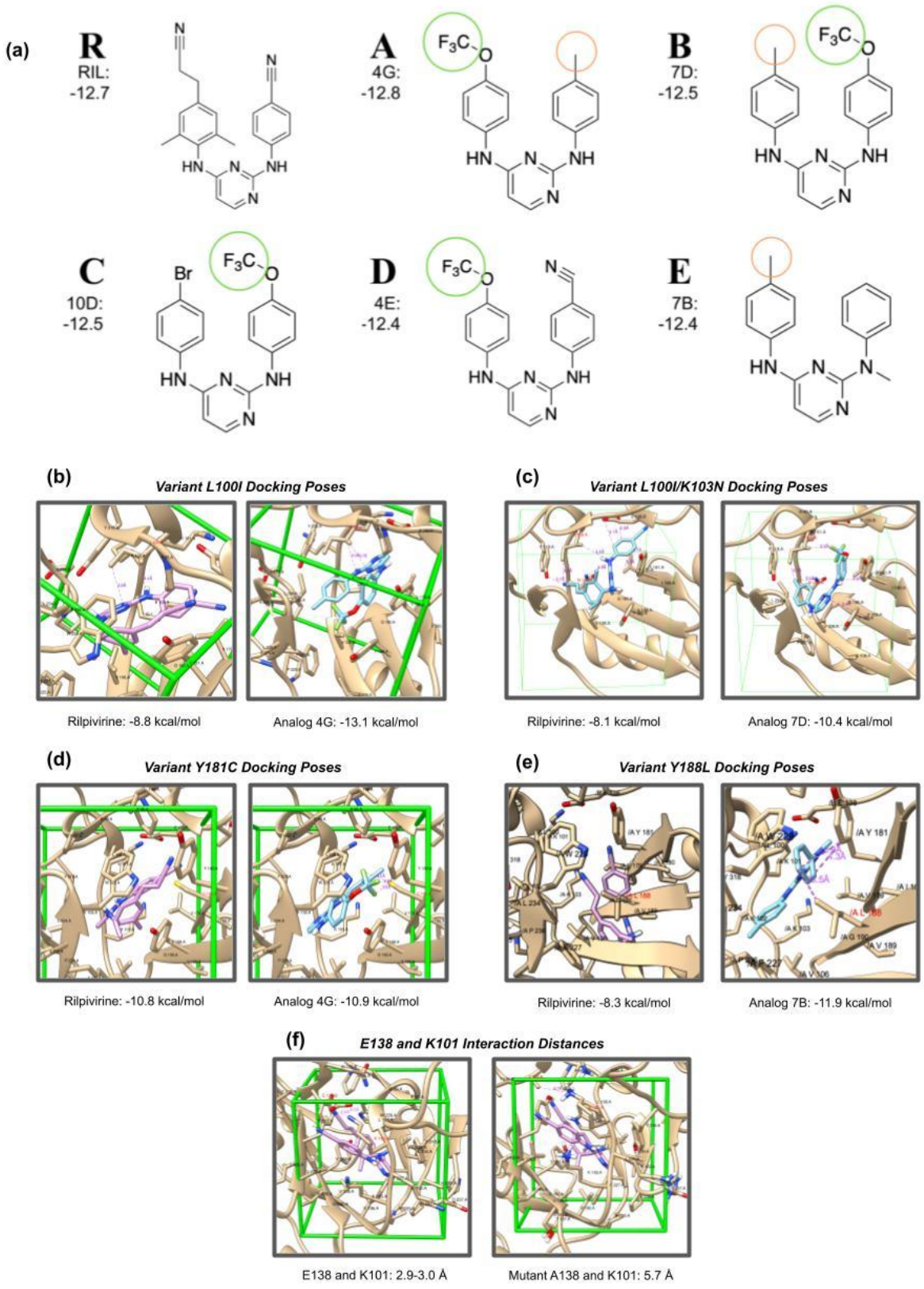

Figure 5. Docking poses of rilpivirine and key analogs against select homology-modeled structural variants of HIV-RT. (a) Chemical structure of rilpivirine and identified analogs screened in this study (b) binding pose of rilpivirine compared to top analog 4G in binding pocket of the L100I variant (c) binding pose of rilpivirine compared to top analog 7D in binding pocket of the L100I/K103N variant (d) binding pose of rilpivirine compared to top analog 4G in binding pocket of the Y181C variant (e) binding pose of rilpivirine compared to top analog 7B in binding pocket of Y188L variant (f) differences in electrostatic interaction distances between WT residues E138 and K101 versus mutant A138 and K101 essential to the tertiary structure of the allosteric binding pocket.

Discussion

A general trend observed is that mutations from aromatic amino acids to aliphatic or nonpolar amino acids cause a significant decrease in binding affinity. Mutations resulting in amino acids with shorter nonpolar side chains cause worse binding affinity. Furthermore, loss of an aromatic ring is the most detrimental, especially the aromatic ring in Y181 and Y188. Specifically, Y181C and Y188L mutations cause steric hindrances between rilpivirine and the binding site and loss of critical π-π interactions between the aromatic rings in rilpivirine and the side chains of tyrosine. In the Y181C/I/V mutants, which are some of the most common NNRTI-resistant mutations, our analogs have binding affinities similar to those of rilpivirine and do not perform better, due to the loss of the proximal aromatic ring of tyrosine 181, which is crucial for halogen-π bonding between the fluorinated analogs and the aromatic ring. Against mutant Y188L, analog 7B retains most of its binding affinity. The residues E138 in the p51 subunit and K101 in the p66 subunit determine the tertiary structure of the NNRTI binding pocket through electrostatic forces. These residues also form electrostatic attractions between the p51 and p66 subunits, stabilizing the tertiary structure of RT [16]. Against E138A/G/K/Q/R mutations, rilpivirine decreases from -12.7 to about -9.3, whereas the analogs retain their binding affinity. Binding of rilpivirine is dependent on the hydrogen bonding to the peptide backbone, and without the electrostatic interactions between E138 and K101, the binding pocket becomes more distorted, causing decreased binding affinity. Our analogs are able to retain their binding affinity even when the electrostatic interactions are lost because they largely rely on halogen-π interactions with tryptophan 229 and tyrosine 181 instead of relying on rilpivirine's amino nitrile bonding. Lysine is a positively charged amino acid, and when K101 mutates to either K101E/G, which are not positively charged, it causes a loss in electrostatic interactions between K101 and E138. Our analogs have a binding affinity significantly better than rilpivirine against the L100I mutation, however, L100I rarely occurs alone; it mostly occurs in combination with K103N, causing over 10-fold reduced susceptibility to rilpivirine [12]. Both L100 and K103 have hydrophobic, fatty tails, which enables hydrophobic interactions with the rilpivirine cyanobenzene. The K103N mutant loses the aliphatic tail which is important for binding affinity. Analog 7D retains better binding affinity than rilpivirine against double mutant L100I/K103N and single mutant K103N, suggesting that hydrophobic interactions with K103 are not overly significant in 7D's binding pose. The other analogs and especially rilpivirine still faced decreased binding affinity.

The number of NNRTI-resistant mutants from prolonged usage of NNRTIs poses a growing threat to the efficacy of antiretroviral therapy. Thus, the continued design and development of novel antiretroviral small molecule therapeutics is paramount to addressing the future of HIV/AIDS. With the capabilities of computational tools available, we can rapidly screen large compound libraries, which is more time and cost-effective than in vitro or in vivo screening. Using biophysical simulations including homology modeling and molecular docking, we have effectively modeled structural variants in RT without having to obtain crystallographic x-ray structures. However, while the results presented herein demonstrate the identification of and provide a structural rationale for hit compounds that retain high binding affinity to several rilpivirine-resistant HIV variants, whether the trends observed in binding affinity correspond with retention of antiretroviral activity remain to be seen. To this end, laboratory syntheses of our top hit compounds are currently underway and in the future we hope this will provide information about the in vitro functional efficacy of the compounds described. Moreover, since the emergence of new viral variants is a continued threat in a variety of viral diseases, we envision that such computational workflows might be similarly employed towards the development of new antiviral compounds to fight such variants.

Methods

Modeling, Design, and Molecular Mechanics Preoptimization

The library of rilpivirine analogs was systematically created and modeled using Avogadro [17], an open-source molecular modeling software package. All chemical entities screened in this study were initially optimized by molecular mechanics using the UFF94 force field at 10,000 steps, as per our previous report.

Density Functional Theory (DFT)

Input files for rigorous quantum-mechanical optimization were created through Avogadro. The geometries of each structure were thermodynamically minimized via density functional theory (DFT) through ORCA [18], an ab initio quantum molecular modeling software, using a B3LYP functional and def2-SVP basis set with a continuum solvation model (CPCM) in water. All DFT calculations were performed on a Dell PowerEdge 710 server with a 24 core Intel Xeon X5660 processor at 2.80 GHz and 32GB RAM.

Molecular Docking

In concordance with our previous report, with a batch script [19] submission to AutoDock Vina [20], optimized structures were docked to the allosteric binding pocket of RT to predict binding affinities of our designed analogs. The unliganded structure of rilpivirine bound to a representative reverse transcriptase of HIV [PDB:3MEE (13)] was used as the receptors and internal standard for comparison. The center atom of rilpivirine was set as the center of a 16 by 16 by 16 Å grid box (Fig. 1). Predicted binding modes were preliminarily judged through the value of free energy of binding (ΔG) in kcal/mol. The final binding poses were visualized through Chimera [21] before the final docking positions and protein-ligand interactions were analyzed to extract both predicted binding thermodynamics and the structural basis for such results (Fig. 5). Molecular docking experiments were performed on a Dell PowerEdge 710

server with a 24 core Intel Xeon X5660 processor at 2.80 GHz and 32GB RAM.

Homology Modeling

The structure of the HIV-1 Reverse Transcriptase in Complex with TMC278 [PDB:3MEE (13)] was used as the wild type (WT) reference sequence from which variants were modeled using ChimeraX (22, 23). backbone-dependent Dunbrack 2010 rotamer library. The models were then checked for clashes between nearby amino acids. HIV-1 RT mutations were taken from the 2019 Update of the Drug Resistance Mutations in HIV-1 [10] and. Homology modeling was performed on the ChimeraX version 1.1 (2020-09-09) suite on a Lenovo ThinkCentre computer with a 4-core Intel I5 processor at 3.20 GHz and 8 GB RAM.

AUTHOR INFORMATION

Corresponding Author

Charissa Luk - charissaluk1@gmail.com

Author Contributions

All authors have given approval to the final version of the manuscript.

Funding Sources

Funds used to support research were supplied through the Olive Children Foundation and its community of corporate sponsors.

ACKNOWLEDGMENT

The authors declare no competing financial interests in the work expressed in this manuscript.

The authors would like to thank Prof. Robert Downing and the computer science department at the Aspiring Scholars Directed Research Program for computational support on the server cluster. We gratefully acknowledge the Olive Children Foundation and its community of corporate sponsors and supporters for funding our research. Last but not least, we thank the Aspiring Scholars Directed Research program for providing us with lab space as well as the opportunity to conduct high-quality research.

ABBREVIATIONS

ATerp, Alpha Terpinene; Berb, Berberine; RBengal, Rose Bengal; MBlue, Methylene Blue; UV, Ultraviolet; TDDFT, Time-Dependent Density Functional Theory; DFT, Density Functional Theory; NMR, Nuclear Magnetic Resonance; DNA, Deoxyribose Nucleic Acid; ppm, parts per million; LED, Light Emitting Diode;

REFERENCES

1. "The Global HIV/AIDS Epidemic." HIV.gov, 7 July 2020, www.hiv.gov/hiv-basics/overview/data-and-trends/global-statistics.
2. "What Are HIV and AIDS?" HIV.gov, 18 June 2020, www.hiv.gov/hiv-basics/overview/about-hiv-and-aids/what-are-hiv-and-aids.
3. HIV Treatment: The Basics. (n.d.). Retrieved January 07, 2021, from https://hivinfo.nih.gov/understanding-hiv/fact-sheets/hiv-treatment-basics
4. Sharp, Paul M, and Beatrice H Hahn. "The evolution of HIV-1 and the origin of AIDS." Philosophical transactions of the Royal Society of London. Series B, Biological sciences vol. 365,1552 (2010): 2487-94. doi:10.1098/rstb.2010.0031
5. Usach, Iris et al. "Non-nucleoside reverse transcriptase inhibitors: a review on pharmacokinetics, pharmacodynamics, safety and tolerability." Journal of the International AIDS Society vol. 16,1 1-14. 4 Sep. 2013, doi:10.7448/IAS.16.1.18567
6. Azijn, Hilde et al. "TMC278, a next-generation nonnucleoside reverse transcriptase inhibitor (NNRTI), active against wild-type and NNRTI-resistant HIV-1." Antimicrobial agents and chemotherapy vol. 54, no. 2, 2010, pp. 718-27. doi:10.1128/AAC.00986-09
7. Molina, J. M., Cahn, P., Grinsztejn, B., Lazzarin, A., Mills, A., Saag, M., ... & ECHO Study Group. (2011). Rilpivirine versus efavirenz with tenofovir and emtricitabine in treatment-naive adults infected with HIV-1 (ECHO): a phase 3 randomised double-blind active-controlled trial. The Lancet, 378(9787), 238-246.
8. Buscher, A et al. "Impact of antiretroviral dosing frequency and pill burden on adherence among newly diagnosed, antiretroviral-naive HIV patients." International journal of STD & AIDS vol. 23, no. 5, 2012, pp. 351-5. doi:10.1258/ijsa.2011.011292
9. Minuto, Joshua J, and Richard Haubrich. "Etravirine: a second-generation NNRTI for treatment-experienced adults with resistant HIV-1 infection." Future HIV therapy vol. 2, no. 6, 2008, pp. 525-537. doi:10.2217/17469600.2.6.525
10. Wensing, A. M., Calvez, V., Ceccherini-Silberstein, F., Charpentier, C., Günthard, H. F., Paredes, R., Shafer, R. W., & Richman, D. D. (2019). 2019 update of the drug resistance mutations in HIV-1. Topics in Antiviral Medicine, 27(3), 111–121. https://pubmed.ncbi.nlm.nih.gov/31634862
11. Wu, J. et al. "Design and in silico screening of analogs of rilpivirine as novel non-nucleoside reverse transcriptase inhibitors (NNRTIs) for antiretroviral therapy." Journal of Emerging Investigators 2021, online.
12. "NNRTI Resistance Notes." NNRTI Resistance Notes - HIV Drug Resistance Database, hivdb.stanford.edu/dr-summary/resistance-notes/NNRTI/.
13. Lansdon, Eric B et al. "Crystal structures of HIV-1 reverse transcriptase with etravirine (TMC125) and rilpivirine (TMC278): implications for drug design." Journal of medicinal chemistry vol. 53, no. 10, 2010, pp. 4295-9. doi:10.1021/jm1002233
14. Pollock, Jonathan, et al. "Rational Design of Orthogonal Multipolar Interactions with Fluorine in Protein–Ligand Complexes." Journal of Medicinal Chemistry, vol. 58, no. 18, 2015, pp. 7465–7474., doi:10.1021/acs.jmedchem.5b00975.
15. Bauer, Matthias R., et al. "Harnessing Fluorine–Sulfur Contacts and Multipolar Interactions for the Design of p53 Mutant Y220C Rescue Drugs." ACS Chemical

Biology, vol. 11, no. 8, 2016, pp. 2265–2274., doi:10.1021/acschembio.6b00315.
16. Smith, Steven J., et al. “Rilpivirine Analogs Potently Inhibit Drug-Resistant HIV-1 Mutants.” Retrovirology, vol. 13, no. 1, 2016, doi:10.1186/s12977-016-0244-2.
17. Hanwell, Marcus D., et al. Journal of Cheminformatics, vol. 4, no. 17, 2012, doi:10.1186/1758-2946-4-17.
18. Neese, Frank. “The ORCA Program System.” WIREs Computational Molecular Science, vol. 2, no. 1, 2011, pp. 73–78. doi:10.1002/wcms.81.
19. Ashok, Bhavesh. “Bhaveshashok/AutoDockVina-BatchSubmission.” GitHub, 2020, github.com/bhaveshashok/AutoDockVina-BatchSubmission.
20. Trott, Oleg, and Arthur J Olson. “AutoDock Vina: improving the speed and accuracy of docking with a new scoring function, efficient optimization, and multithreading.” Journal of computational chemistry, vol. 31, no. 2, 2010, pp. 455-61. doi:10.1002/jcc.21334
21. Pettersen, Eric F et al. “UCSF Chimera--a visualization system for exploratory research and analysis.” Journal of computational chemistry, vol. 25, no. 13, 2004, pp. 1605-12. doi:10.1002/jcc.20084
22. UCSF ChimeraX: Structure visualization for researchers, educators, and developers. Pettersen EF, Goddard TD, Huang CC, Meng EC, Couch GS, Croll TI, Morris JH, Ferrin TE. Protein Sci. 2021 Jan;30(1):70-82.
23. UCSF ChimeraX: Meeting modern challenges in visualization and analysis. Goddard TD, Huang CC, Meng EC, Pettersen EF, Couch GS, Morris JH, Ferrin TE. Protein Sci. 2018 Jan;27(1):14-25